SANDIA REPORT

SAND2015-9610
Unlimited Release
Printed November 2015

Feasibility of Observing and Characterizing Single Ion Strikes in Microelectronic Components

R. Dingreville, K. Hattar, D. Bufford

Prepared by
Sandia National Laboratories
Albuquerque, New Mexico 87185 and Livermore, California 94550

Sandia National Laboratories is a multi-program laboratory managed and operated by Sandia Corporation, a wholly owned subsidiary of Lockheed Martin Corporation, for the U.S. Department of Energy's National Nuclear Security Administration under contract DE-AC04-94AL85000.

Sandia National Laboratories

Issued by Sandia National Laboratories, operated for the United States Department of Energy by Sandia Corporation.

Available to DOE and DOE contractors from
U.S. Department of Energy
Office of Scientific and Technical Information
P.O. Box 62
Oak Ridge, TN 37831

Telephone: (865) 576-8401
Facsimile: (865) 576-5728
E-Mail: reports@adonis.osti.gov
Online ordering: http://www.osti.gov/bridge

Available to the public from
U.S. Department of Commerce
National Technical Information Service
5285 Port Royal Rd
Springfield, VA 22161

Telephone: (800) 553-6847
Facsimile: (703) 605-6900
E-Mail: orders@ntis.fedworld.gov
Online ordering: http://www.ntis.gov/help/ordermethods.asp?loc=7-4-0#online

SAND2015-9610
Unlimited Release
Printed November 2015

Feasibility of Observing and Characterizing Single Ion Strikes in Microelectronic Components

Rémi Dingreville
Org. 06233
Sandia National Laboratories
Albuquerque, NM 87185-MS0747
rdingre@sandia.gov

Khalid Hattar
Org. 01111
Sandia National Laboratories
Albuquerque, NM 87185-MS1056
khattar@sandia.gov

Daniel Bufford
Org. 01111
Sandia National Laboratories
Albuquerque, NM 87185-MS1056
dcbuffo@sandia.gov

Abstract

The transient degradation of semiconductor device performance under irradiation has long been an issue of concern. A single high energy charged particle can degrade or permanently destroy the microelectronic component potentially altering the course or function of the systems. Disruption of the the crystalline structure through the introduction of quasi-stable defect structures can change properties from semiconductor to conductor. Typically, the initial defect formation phase is followed by a recovery phase in which defect-defect or defect-dopant interactions modify the characteristics of the damaged structure.

In this LDRD Express, in-situ ion irradiation transmission microscopy (TEM) in-situ TEM experiments combined with atomistic simulations have been conducted to determine the feasibility of imaging and characterizing the defect structure resulting from a single cascade in silicon. In-situ TEM experiments have been conducted to demonstrate that a single ion strike can be observed in Si thin films with nanometer resolution in real time using the in-situ ion irradiation transmission electron microscope (I^3TEM). Parallel to this experimental effort, ion implantation has been numerically simulated using Molecular Dynamics (MD). This numerical framework provides detailed predictions of the damage and follow the evolution of the damage during the first nanoseconds.

The experimental results demonstrate that single ion strike can be observed in prototypical semiconductors.

Acknowledgments

This work was funded by the Laboratory Directed Research and Development (LDRD) program at Sandia National Laboratories. We gratefully acknowledge support of the Radiation Effects and High Energy Density Sciences (REHEDS) LDRD committee. We would like to thank Sarah Blair for her help with the experiments.

Contents

List of Figures

List of Tables

Nomenclature

ACD Anti-Contamination Device

FIB Focused Ion Beam

I^{3}TEM In-situ ion Irradiation Transmission Electron Microscope

IBL Ion Beam Laboratory

LDRD Laboratory Directed Research & Development

MD Molecular Dynamics

PKA Primary Knock on Atom

REHEDS Radiation Effects and High Energy Density Sciences

SNL Sandia National Laboratories

TEM Transmission Electron Microscope

1. Introduction

Radiation induced displacement damage is an issue in many applications including nuclear reactors, space electronics, and nuclear weapons microelectronics. Of particular interest, ion implantation is a technique widely used in the semiconductor industry to introduce impurities into silicon wafers both because of the control it affords over doping conditions and because it can be performed at low temperatures [11].

Ion implantation generates significant damage in silicon devices, and this damage depends on factors such as the implanted ion species, dose, and implant temperature and energy [7, 11]. When energetic ions strike a silicon substrate they create zones of disorder. The lattice in these defective regions exhibits different damage configurations, going from isolated point defects or point defect clusters surrounded by crystalline silicon, to continuous amorphous layers. The damage generation in each implantation cascade is usually described by the number of displaced atoms or Frenkel pairs. These elementary defects, Si interstitials (I) and vacancies (V), are mobile and interact with each other. The coalescence of Si interstitials results in small Si interstitial clusters, rod-like defects or dislocation loops [4]. Analogously, the interaction among vacancies may lead to the formation of vacancy clusters and voids [8]. When Si interstitials interact with vacancies, it is traditionally assumed that they immediately recombine [12].

Disruption of the crystalline structure due to displacement damage and its evolution in time can alter the structure, band-gap, and electrical properties of these materials [11, 13, 14]. After the cascade is done (picoseconds), the resulting defects will diffuse and interact over timescales from nanoseconds to the life time of the device affecting the material properties and reliability.

However, a direct correlation between the discrete and stochastic nature of radiation damage and the resulting change in properties at the device-level remains an open question due to constraints associated with the experimental techniques and modeling methodologies that are currently available. The ability to understand the mechanisms of defect formation and removal would allow future development of more efficient procedures for silicon wafer manufacturing. This work aims to characterize defect formation in silicon after irradiation with heavy ions using both in-situ transmission electron microscope (TEM imaging) and computational modeling. Section 2 describes the experiments conducted while Section 3 presents results obtained from the atomistic modeling. The outcome of this work established the feasibility of imaging and characterizing the defect structure resulting from a single cascade in Si.

2. In-situ TEM: Characterization of defect formation in silicon after irradiation with heavy ions

2.1 In-Situ Ion Irradiation TEM (I^3TEM)

The experiments we conducted using the Ion Beam Laboratory (IBL) modified TEM that has been developed for examining the underlying mechanisms controlling materials' response to extreme conditions with nanometer resolution. The major components of the I^3TEM facility include: a 200 kV JEOL 2100(HT) TEM, a 6 MV EN Tandem Van de Graaff?Pelletron accelerator, and a 10 kV Colutron G-1 ion accelerator. The 6 MV Tandem and 10 kV Colutron are connected to the I^3TEM perpendicularly to the electron beam through a single custom made electrically isolated and mechanically dampened port to ensure the highest resolution possible during in situ TEM experiments. By flowing D_2 and He beams into the Colutron during concurrent heavy ion irradiation, a limited triple beam condition can be achieved in either the TEM or the larger ex situ multi- beam chamber directly upstream of the TEM.

2.2 TEM sample preparation

TEM samples were prepared from a 50-μm-thick (1 0 0) silicon wafer (Virginia Semiconductor, Fredericksburg, VA) using the small-angle cleavage technique [9]. The silicon wafer was first scribed and cleaved along a [1 2 0] plane approximately 18° from the wafer's primary [1 1 0] cleavage plane, then cleaved along the standard [1 1 0] plane. Cleaving along these planes left a thin pointed wedge of silicon, the points and edges of which were electron-transparent. The small-angle cleavage technique results in only a thin (approximately 1 nm) amorphous native SiO_2 layer on the sample surface. This surface quality is in contrast to ion milling and focused ion beam (FIB) milling methods, which leave thicker surface layers (5-20 nm) of ion damaged and redeposited Si, along with potential Ar or Ga impurities [10]. These wedges were then glued onto 3-mm copper TEM slot grids using a conductive epoxy.

Samples were loaded in a double tilt holder, and examined in a JEOL 2100 TEM operated at 200 kV. For in situ ion irradiation experiments the samples were tilted to +30° in α, and then a few degrees in β to a nearby down-zone imaging condition.

2.3 Results

Samples were irradiated in Sandia's In Situ Ion Irradiation TEM (I^3TEM) facility [6]. Two beam energies were selected for this study: 46 keV Au^{1-} and 1.8 MeV Au^{3+}. Both the damage profiles and types of damage introduced by these beams are different, as will be discussed later. Beam currents used were approximately 5×10^8 ions $cm^{-2}s^{-1}$ with the 46 keV beam and 1.7×10^9 ions $cm^{-2}s^{-1}$. Images collected at approximately 4.5 frames per second.

SRIM (Stopping Range of Ions in Matter [16]) simulations were performed to estimate the damage profiles of each beam. These were run in the "quick" damage calculation mode, with an angle of incidence 60° from normal (similar to the experimental setup), and 100 nm target layer thickness specified (representative of a typical TEM sample). SRIM simulations estimated total damage within the sample thickness from each beam at 820 and 8000 vacancies ion^{-1} for the 46 keV and 1.8 MeV beams, respectively. We note that these are on average, and take into account both ionization and displacement damage throughout the layer (Fig. 2.1). Since the estimated end of range for 46 keV Au is less than 30 nm, the damage is localized near the surface. The ratio of nuclear to electronic stopping power is 6 for 46 keV Au and 1.4 for 1.8 MeV Au in Si.

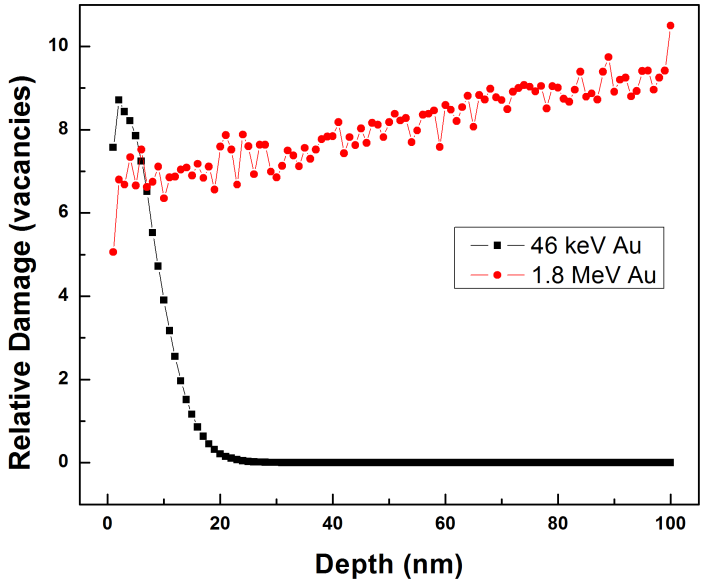

Figure 2.1. Damage profiles for 46 keV and 1.8 MeV Au in Si, as predicted by SRIM.

The cleaved Si samples were found to be of good quality, as see in Fig. 2.2. Although dislocations were left in some areas from the cleavage process, these were typically spaced broadly

enough that the areas in between could be observed. Si samples were examined with and without the anti-contamination device (ACD), a liquid nitrogen cold finger in the TEM designed to reduce electron beam enhanced deposition of carbon on the sample surface. Carbon deposition and an accompanying gradual decrease in image quality were evident without the ACD. Given the small expected defect cluster size, the ACD was utilized for all experiments included here.

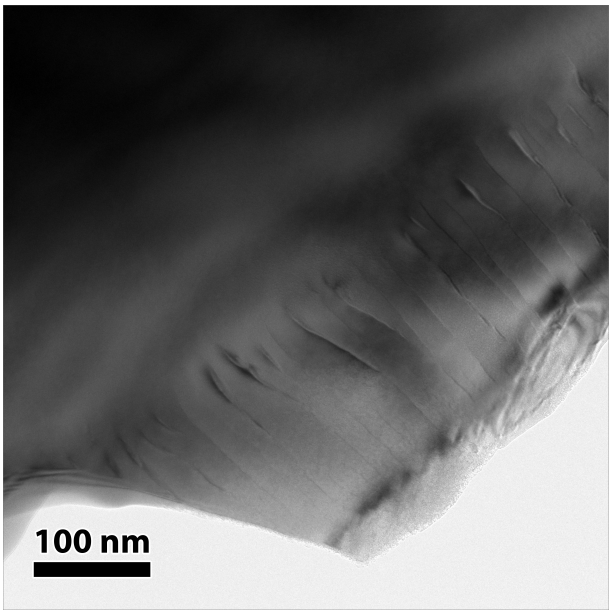

Figure 2.2. Overview of a cleaved edge of a Si sample before irradiation. Long parallel dislocations from the cleaving process are apparent, but otherwise little damage was present.

Imaging during experiments was performed at higher magnifications in order to better resolve the irradiation-induced defect clusters. For example, Fig. 2.3(a) shows the Si sample at 100,000 $\times$ magnification. The ion fluxes discussed earlier were selected so that single ions arrived in the viewing area, spaced a few seconds temporally. In the case of Fig. 2.3, the flux corresponded to 1 ion approximately every 6 s in the 170 nm $\times$ 170 nm area shown. This arrangement ensured that the observed events and resulting damage were indeed due to single ions.

Defect clusters caused by single ion events were resolved in the video collected in situ, as demonstrated in Fig. 2.3. Here, the sample has been tilted to + 30° in α, and is in a down-zone imaging condition near a [$\bar{1}$ 1 2]-type zone axis. Panels (a) and (b) show defect cluster formation from a single ion event. These panels are sequential frames from the TEM video spaced 0.22 s apart. From the initial panel in (a), a defect cluster appears in (b), indicated by an arrow. This new feature is somewhat difficult to see clearly in the raw micrograph, but can be seen better in (c). This panel is an inverse image, constructed by combing panel (a) and the inverse of panel (b). Here, any features that are in both (a) and (b) appear as a flat grey field. Features that appear in (b)

but not (a) are darker, as evidenced by the defect cluster. Conversely, features that appear in (a) but not (b) would appear lighter, but no such changes took place in this sequence. The defect cluster was roughly circular in this projected view, with a diameter of approximately 3.3 nm.

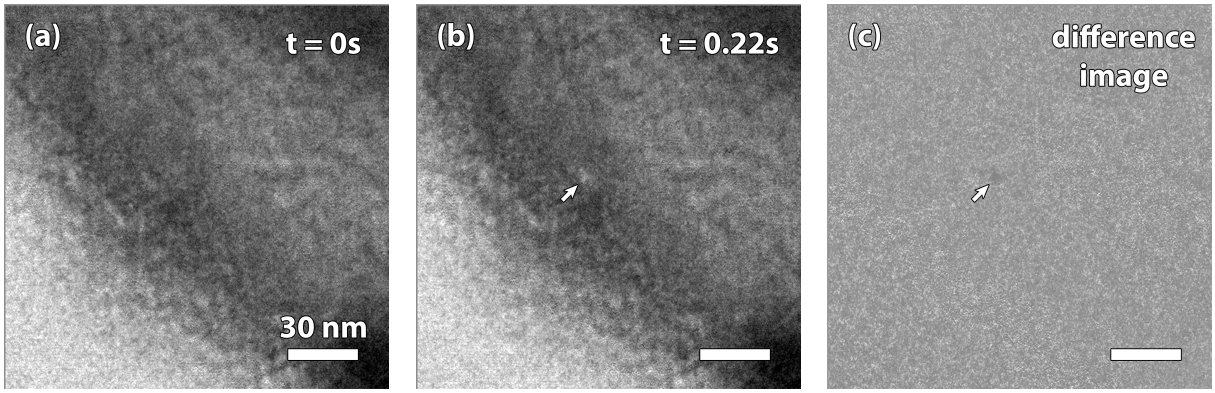

(a) (b) (c)

Figure 2.3. Individual frames taken from video collected in situ in the TEM during irradiation of the Si sample with 46 keV Au^{-1}. The sample was in a down-zone imaging condition near a [$\bar{1}$ 1 2]-type zone axis. Frames (a) just before and (b) just after a single ion event, with the defect cluster produced marked by the arrow. In the difference image (c), features present in (a) but not (b) appear dark, while unchanged areas appear as a flat grey field. This serves to highlight the newly formed defect cluster more clearly than in the as-collected micrographs.

Figure 3.1 represents a second single ion event sequence similar to that shown in Fig. 2.3, but with 1.8 MeV Au irradiation. Here the sample was again tilted to + 30° in α and was near a down-zone imaging condition about a [$\bar{1}$ 2 3]-type axis. Note that the magnification was greater than in Fig. 2.3, however the higher applied flux resulted in an estimated 1 ion every 10 s in the viewing area, comparable to the other experiment. Again a defect cluster appeared in less than one frame. Here, the defect cluster had an elongated appearance, approximately 6.9 nm and 2.6 nm along the major and minor axes.

Most defect clusters like these were stable after formation, although a few eventually disappeared. Similar defect clusters have been reported to recrystallize due to annealing at a range of temperatures beginning as low as 70 °C [5]. Given that the irradiations were performed at room temperature, there may have been some effects from the electron beam. It is also possible that the clusters in question may have been mobile defects and/or near to the surface, in which case, escape from the sample surface could be the mechanism.

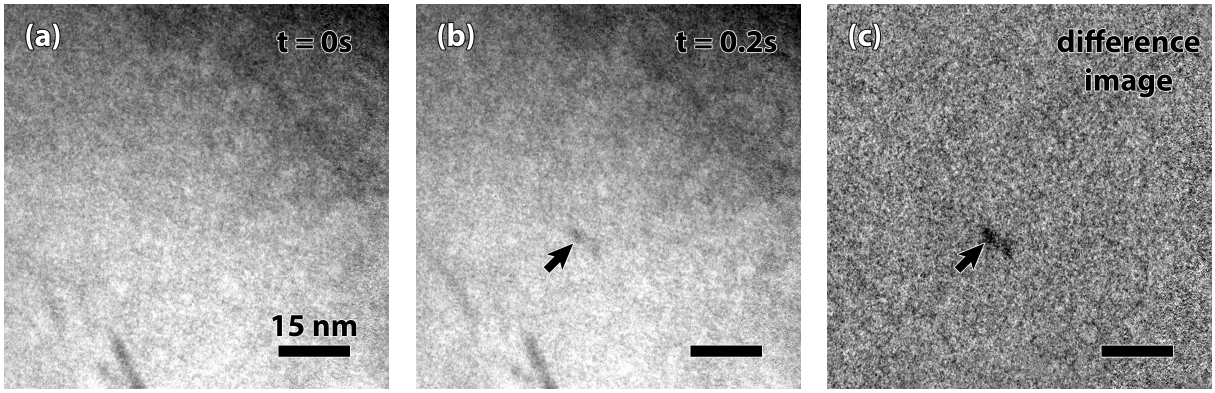

(a) (b) (c)

Figure 2.4. Individual frames taken from video collected in situ in the TEM during irradiation of the Si sample with 1.8 MeV Au^{3+}. The sample was in a down-zone imaging condition near a [$\bar{1}$ 2 3]-type zone axis. Similarly to Fig. 2.3, frames (a) and (b) show the sample just before and just after a single ion event, respectively, with the arrow again marking the new defect cluster. The difference image (c) more clearly highlights the defect cluster, by presenting features in (a) but not (b) as darker, while unchanged areas appear as a flat grey field.

3. Atomistic modeling of defect formation in silicon

Understanding the links between material, radiation conditions, radiation damage accumulation, and changes in material properties. Modeling tools must operate at scales ranging from atomistic to macroscopic in order to investigate these links and predict material property changes in irradiated materials. In this LDRD Express we have simulated the motion and clustering of vacancies and interstitials in silicon using molecular dynamics (MD) methods.

Classical MD simulations were used to simulate collision cascades. Periodic boundary conditions were applied to the fixed-size simulation cells, which contain 1728000 atoms. The temperature of the cell was set to 300 K. The forces acting between the atoms were described with a Tersoff potential with a close-separation pairwise modification based on a Coulomb potential and the Ziegler-Biersack-Littmark universal screening function [15]. The Tersoff interatomic potential describes most Si bonding types quite well, and has many other features [2]. A Langevin thermostat has been applied to dump the subsequent shockwave induced by the primary knock on atom (PKA).

The collision cascades were initiated by giving one of the atoms in the lattice a recoil energy of 10 keV. The initial velocity direction of the recoil atom was chosen randomly. To obtain representative statistics, 5 simulations were conducted. The evolution of each cascade was followed for 50 ps. The electronic stopping power was included in the runs as a nonlocal frictional force affecting all atoms.

Interstitials and vacancies were recognized in the simulations using a Wigner-Seitz cell analysis of the atom positions with respect to the lattice defined by undisturbed simulation cell regions [1]. A lattice site with an empty Wigner-Seitz cell was labeled a vacancy and a cell with multiple atoms an interstitial.

The understanding of the initial states of damage produced by irradiation of Si relies mainly on computer simulations so far since the time scale of the experiments described in the previous section is so far too coarse to capture the initial evolution of radiation induced defects. Consistent with observations made in past studies, initial defect evolution can be summarized as follows. Replacement collision sequences have been shown to be very short in Si due to the lack of close-packed directions in the diamond crystal structure [3] while defects outside the damage zones tend to be predominantly interstitials. Figure **??** illustrates the formation of a defect cluster in a 10 keV cascade in Si.

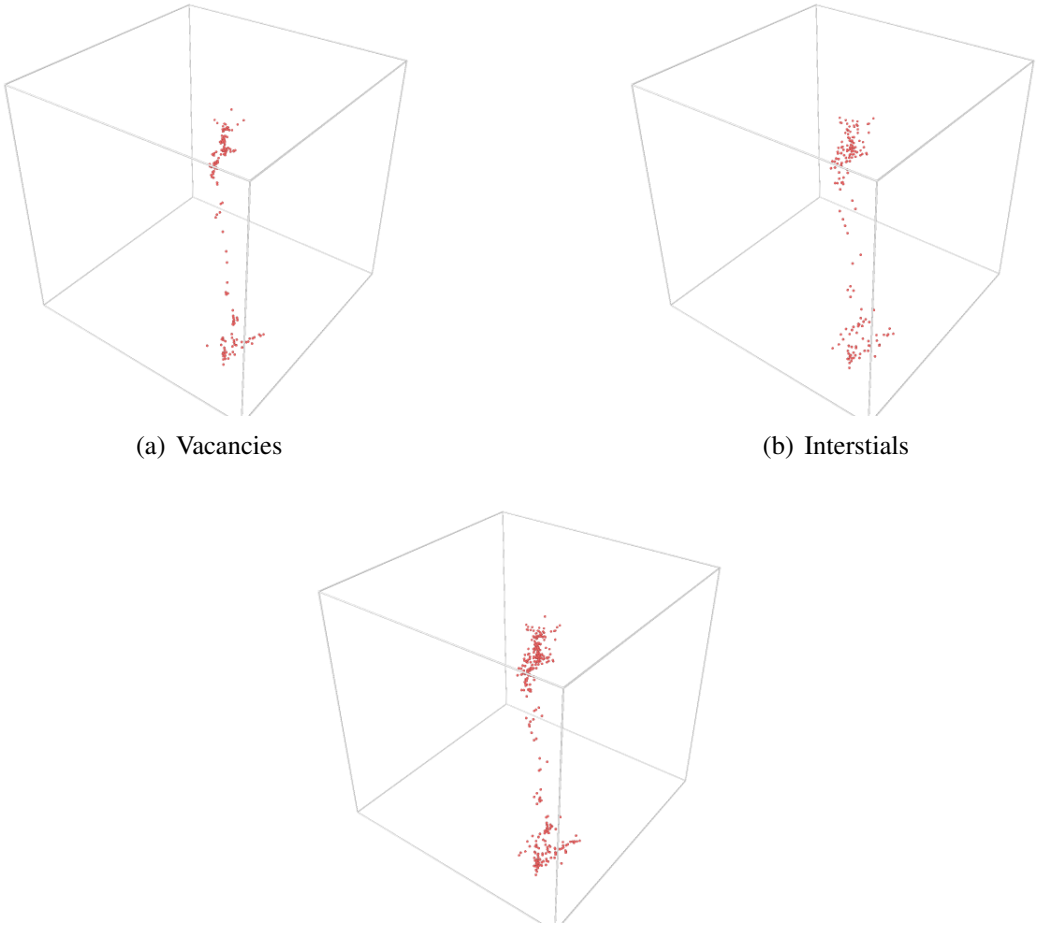

(a) Vacancies

(b) Interstials

(c) Cascade trace

Figure 3.1. Formation of a defect cluster in a 10 keV cascade in Si. The positions of atoms in the cluster correspond to the end of the simulation (50 ps).

4. Summary

The unique capabilities of the In Situ Ion Irradiation TEM at Sandia have been utilized to directly observe displacement damage due to single ion events at near atomic resolution. These experiments have been combined with preliminary defect recombination models (MD) to explain the time evolution of the damage cascades. Three outcomes are drawn from this study:

- Promising experimental results show that single ion strike can be observe within a TEM over long period of times.
- Preliminary modeling results show that a quantification of the type and distribution of defects is straight forward and complementary to the experiments.
- This preliminary study resulted in a full LDRD that has been awarded for the FY16–FY18 period: the I3TEM capabilities will be expanded to cover the important temporal scales ranging from nanoseconds to hours. We will also combine modern TEM image analysis models with defect recombination models to explain the time evolution of the damage cascades.

References

[1] Neil W Ashcroft and N David Mermin. Solid state physics (holt, rinehart and winston, new york, 1976). *There is no corresponding record for this reference*, pages 490–495, 2005.

[2] H. Balamane, T. Halicioglu, and W.A. Tiller. Comparative study of silicon empirical interatomic potentials. *Physical Review B*, 46(4):2250, 1992.

[3] M.J. Caturla, T.D. de la Rubia, G.H. Gilmer, R.J. Culbertson, et al. Materials synthesis and processing using ion beams. In *MRS Symposia Proceedings*, number 316, page 111, 1994.

[4] F. Cristiano, B. Colombeau, and A. Claverie. Energetics of extrinsic defects in Si and their role in nonequilibrium dopant diffusion. In *Defect and Diffusion Forum*, volume 183, pages 199–206. Trans Tech Publ, 2000.

[5] P.D. Edmondson, S.E. Donnelly, and R.C. Birtcher. Amorphisation and recrystallisation of nanometre sized zones in silicon. In *Solid State Phenomena*, volume 108, pages 145–150. Trans Tech Publ, 2005.

[6] K. Hattar, D.C. Bufford, and D.L. Buller. Concurrent *in situ* ion irradiation transmission electron microscope. *Nuclear Instruments and Methods in Physics Research Section B: Beam Interactions with Materials and Atoms*, 338:56–65, 2014.

[7] K.S. Jones, S. Prussin, and E.R. Weber. A systematic analysis of defects in ion-implanted silicon. *Applied Physics A*, 45(1):1–34, 1988.

[8] A.P. Knights, F. Malik, and P.G. Coleman. The equivalence of vacancy-type damage in ion-implanted Si seen by positron annihilation spectroscopy. *Applied Physics Letters*, 75(4):466–468, 1999.

[9] J.P. McCaffrey. Small-angle cleavage of semiconductors for transmission electron microscopy. *Ultramicroscopy*, 38(2):149–157, 1991.

[10] J.P. McCaffrey, M.W. Phaneuf, and L.D. Madsen. Surface damage formation during ion-beam thinning of samples for transmission electron microscopy. *Ultramicroscopy*, 87(3):97–104, 2001.

[11] K.H. Nicholas. Implantation damage in silicon devices. *Journal of Physics D: Applied Physics*, 10(4):393, 1977.

[12] L. Pelaz, M. Jaraiz, G.H. Gilmer, H.-J. Gossmann, C.S. Rafferty, D.J. Eaglesham, and J.M. Poate. B diffusion and clustering in ion implanted Si: The role of B cluster precursors. *Applied Physics Letters*, 70(17):2285–2287, 1997.

[13] R. Radu, I. Pintilie, L.C. Nistor, E. Fretwurst, G. Lindstroem, and L.F. Makarenko. Investigation of point and extended defects in electron irradiated silicon – Dependence on the particle energy. *Journal of Applied Physics*, 117(16):164503, 2015.

[14] P.J. Schultz, C. Jagadish, M.C. Ridgway, R.G. Elliman, and J.S. Williams. Crystalline-to-amorphous transition for Si-ion irradiation of Si (100). *Physical Review B*, 44(16):9118, 1991.

[15] J.F. Ziegler, J.P. Biersack, and U. Littmark. *The stopping and range of ions in matter*, volume 1. Springer, 1985.

[16] J.F. Ziegler, M.D. Ziegler, and J.P. Biersack. SRIM – The stopping and range of ions in matter. *Nuclear Instruments and Methods in Physics Research Section B: Beam Interactions with Materials and Atoms*, 268(11):1818–1823, 2010.

DISTRIBUTION:

1	MS 1056	D. Bufford, 1111
1	MS 1056	J. Custer, 1111
1	MS 1056	K. Hattar, 1111
1	MS 0744	Patrick D. Mattie, 6233
1	MS 0747	R. Dingreville, 6233
1	MS 0899	Technical Library, 9536 (electronic copy)

Sandia National Laboratories